Journal of Solid Mechanics Vol. 14, No. 2 (2022) pp. 171-189
DOI: 10.22034/jsm.2021.1924081.1683

Fatigue Life Analysis of the Propeller Shafting System of a VLCC Ship Powertrain System Using Finite Element or Distributed-Lumped Methods

A. Gholami [1], S.A. Jazayeri [2,*], Q. Esmaili [3]

[1]*Department of Mechanical Engineering, Ayatollah Amoli Branch, Islamic Azad University, Amol, Iran*
[2]*Department of Mechanical Engineering, K. N. Toosi University of Technology, Tehran, Iran*
[3]*School of Engineering Technology, University of Special Modern Technologies, Amol, Iran*

Received 13 February 2022; accepted 2 April 2022

ABSTRACT

In this study, the dynamic behavior of the propulsion system of a VLCC (Very Large Crude oil Carrier) ship is investigated using a multi-input multi-output model. In this system the engine ordered speed and the number of active cylinders are assumed as inputs and the dynamic parameters of the engine such as torque and speed are considered as outputs. In this research, the effects of sea wave and wind on the system dynamic behavior have been investigated. In addition, the ship powertrain system is investigated in which the intermediate shaft and propeller shaft are analyzed using lumped parameter method, finite element method, distributed-lumped method and the results of these modeling techniques are compared to the modeling results in which the connecting shafts were considered as rigid body. Comparison of the results shows that there are significant differences between the results of rigid body method and other three types of system modeling. On the other hand, the time required to run the distributed-lumped model is much shorter compared to other methods that are considered in the study for the dynamic behavior of the ship's powertrain systems. On the other hand, the fatigue analysis of the ship power transmission shafts shows that the fatigue life assessment of these shafts is of great importance and should be considered in the design phase.

Keywords: Ship propulsion system modeling; Distributed-Lumped; Fatigue analysis; MVEM (Mean Value Engine Model); Finite element.

1 INTRODUCTION

LACK of full knowledge to work in unpredicted weather conditions, especially against waves, has caused ships to be designed and optimized for calm water conditions. Despite doing our best to design ships to be safe, shipping operations face risks on rough waters. Today, apart from optimizing and managing the activity of vessels

*Corresponding author.
E-mail address: sajazayeri@hotmail.com (S.A. Jazayeri)

when dealing with waves, also energy consumption and efficiency of ships are of great importance. Fuel price fluctuations, competing rental costs and strict environmental regulations have a major impact on the activities of shipping companies [1,2]. As mentioned, due to complexity of system, ship propulsion is currently designed for calm water condition, and for rough water conditions, usually excess15-25% of the energy required in calm water conditions is considered as a good sea margin to cover those conditions. Therefore, at the engine selection phase of the ship's propulsion system, the sea margin must be considered in such a way that even in worse weather conditions, the minimum possible engine power ensures the performance and safety of the ship. The wave effects on the ship's propulsion system are still unknown. However, the ship propulsion system reacts to the flow field variations in the waves, and therefore it is necessary to consider the effects of the waves on the ship powertrain system, especially at the design stage. When part or all of the ship's propeller comes out of the water, its resistance torque will be significantly reduced, and depending on the type of engine control system, there would be a tendency of sudden change in propeller speed. As a result, it is important to study the dynamics of the ship's powertrain system in the face of waves. Several researchers have studied and compared the propulsion parameters of a ship in waves and calm water. Nakamura and Naito [3] and Amini [4] studied the effects of ship motion and waves on wake fractions, thrust deduction, and finally changes in thrust and propeller torque. The movement of the ship increases the average wake and the resulting oscillations [5, 6]. Using the Reynolds Averaged Navier Stokes equations (RANS) simulation, Gao et al. [7] investigated the wake field in the presence of waves and the motion of the ship and modeled the nominal wake field in the waves. Taskar et al. [8] studied the changes in propeller emergence and submergence in the waves and its effects on engine load. These researches showed that the presence of an unsteady inflow to the ship propeller will increase engine fuel consumption. There is a fact that the presence of variable loads on the ship propeller in the waves can cause system failure, so it is necessary to predict these loads at the design stage [4]. Extensive research and full-scale experiments performed by Kayano et al. [9] show that the delivered power of the propulsion system, measured in the presence of wind and waves, is higher than estimated value. As a result, considering the effects of wind and waves in energy consumption calculations is very important. The study of engines as an important part of the ship propulsion system is of great importance. Engine models can be classified into transfer function models [10], cycle Mean Value Engine Models (MVEMs)[11,12] , zero or one-dimensional models [13], and multi-zone phenomenological models [14]. In a transfer function model, which usually represents the relationship of fuel consumption to engine speed, the essential characteristics of the system is not reflected. On the other hand, more accurate results can be achieved using multidimensional models, but achieving these results will be much more time consuming and computationally costly. The most commonly used models are zero-dimensional models that require a large number of input data and takes longer time to run. However, these models can far more accurately predict the performance of the engine. On the other hand, the cycle mean value engine models are less complex and require a limited number of inputs and their execution time is much more reasonable with sufficient accuracy. The basic assumption in the cycle mean value engine modeling method is that the air and fuel flows to the cylinder are continuous, so the periodic trend of the engine cylinder processes is ignored and therefore this approach can factorize the engine cycle as the mean time change of factors, while the in-cycle variation (e.g. per degree of crank angle) is not determined [15].

In mechanical systems modeling, using the lumped parameter method is the simplest approach in which the elements are making up the system have point-wise and concentrated effects, therefore using this technique reduces the accuracy of design and modeling processes [16]. In order to improve the accuracy, numerical methods such as finite element methods are employed. The basic assumption of FEM is that the dynamic system comprises a finite number of elements [17]. Increasing the number of elements may lead to higher computational costs and time. In distributed modeling as an analytical method, fundamental assumption is that the dynamic system comprises an infinite number of elements that are infinitesimal. Hybrid (Distributed-Lumped) model is a combination of lumped and distributed models of assemblies that exist in the dynamic systems. Implementing the D-L model in software environments such as Simulink is relatively easy with the benefit of lower computational costs. Ship powertrain system is not a concentrated unit so that the masses, stiffness, inertias and so on are distributed over wide distances of length with point-wise concentrated elements such as flywheel, gearbox, coupling and bearing installed in the system. Ships powertrain systems are usually modeled using purely lumped where, in reality, the propulsion systems are neither specifically lumped nor distributed. These systems are combination of lumped and distributed elements. Murawski and Charchalis [18] investigated the torsional vibrations of a ship power transmission system that is induced by the internal and external loads such as engine torque, propeller outputs, hull deformation and other kinds of excitations, using finite element method and showed that in overload operation will result fracture and failure of the marine propulsion shaft. Also other research approach such as transfer matrix method [19], finite element method [20], energy method [21], wave approach method [22] and lumped-mass method [23] were used to analyze the ship propulsion shaft behavior dynamically. It worth to emphasis that many of these models do not have the

flexibility to consider modeling parameters such as system geometry, stiffness and damping coefficients, therefore the modeling process using these methods could become complex at a time. Grzadziela analyzed vibration of the propeller shaft of a naval ship in the Ansys environment and modeled underwater detonation effects using Lagrange equation to achieve a diagnostic oriented model [24]. Kluczyk and Grzadziela [25] presented the vibration analysis of a warship powertrain system elements using methods of processing vibration signal such as FFT analysis to perform a proper diagnosis of vibration.

In this study, the performance of the propulsion system of a Very Large Crude oil Carrier (VLCC) are investigated using the results determined by a modular model built in Matlab/Simulink. The modular model is block-oriented so that the model is made by special blocks for each component. The various parts of the propulsion system such as engine, ship hull, propeller and shafting system are represented by separate blocks, while suitable interfaces and connections are used to exchange the specified factors between the blocks. The engine is modeled using cycle mean value engine model (MVEM) in which the exhaust and scavenging receivers are thermodynamically modeled as open systems. Equations containing dimensionless coefficients of torque and thrust are used to model the ship's propeller, while the ship dynamics equations are used to determine the ship's speed and longitudinal movement. The effects of wave have been investigated in this study. In addition, the ship propulsion system behavior has been modeled using lumped parameter method, finite element method, Hybrid (Distributed-Lumped) modeling technique. Finally, the results of these models are presented and compared with each other as well as in the case where the shaft is considered as a rigid body system. The results show that the use of distributed-lumped technique increases the accuracy of ship powertrain system dynamic analysis and decreases computational time significantly compared to other methods and can be used as an effective tool in system design.

2 SHIP MODEL DESCRIPTION

2.1 Engine model

The quasi-steady, cycle mean value method is used for engine thermodynamic modeling for ship simulation. The basic premise of quasi-steady model is that the equations used for steady-state analysis can be extended to transient conditions [26]. In this model, the cycle–averaged temporal mechanical and thermodynamic variables, from cycle to cycle of the engine, are estimated. Consequently, changes in the cycle and in-cylinder parameters (e.g. per degree of crank angle) is not determined. This model contains scavenging and exhaust receivers, cylinders, turbocharger, air cooler and exhaust pipe. As early mentioned, the basic assumption in this model is that the fuel and air flowing into the cylinders are continuous in addition to the scavenging and exhaust receivers are thermodynamically open systems.

Engine performance is calculated using following equations [26,27]:

$$Q_e = \frac{p_b V_D}{2\pi rev_{cy}} \tag{1}$$

$$P_b = \frac{\pi Q_e N_e}{30} \tag{2}$$

$$p_b = \frac{60 P_b}{z_{cyl} V_D N_e} \tag{3}$$

where P_b is the engine brake power (watts), p_b is the engine brake mean effective pressure (BMEP), N_e is the engine crankshaft rotational speed (*rpm*), Q_e is the engine torque, rev_{cy} is revolutions per cycle (2 for four-stroke engine) and V_D is the engine displacement volume. The mass flow rate (*kg/s*) of fuel injected is calculated as follows:

$$\dot{m}_f = \frac{z_{cyl}\, m_{fcycle}\, N_e}{(60\ rev)} \tag{4}$$

where z_{cyl} is the number of engine cylinders, m_{fcycle} is the mass of the fuel injected per cylinder per cycle and considered to be a function of the fuel index (rack) position (F_R):

$$m_{fcycle} = m_{fmax} F_R \tag{5}$$

where m_{fmax} is the maximum amount of fuel that can be injected into a cylinder in one cycle. The fuel index position (F_R) is represented in a non-dimensional shape and is within the interval [0,1] that value 1 corresponds to the engine maximum continuous rating (MCR).

The engine crankshaft rotational speed variations per time ($\dot{N}_e$) is calculated using angular momentum conservation in the powertrain system:

$$\dot{N}_e = \frac{30}{\pi}\left(\frac{Q_e - Q_p}{I_{shaftline}}\right) \tag{6}$$

where $I_{shaftline}$ is the sum of mass moments of the inertia of the shafting system, engine and propeller(with entrained water), Q_e is the output engine torque, and Q_p is the propeller torque.

A proportional-integral (PI) controller is used for the engine governor to adjust the fuel index as follows:

$$u = u_0 + k_p \Delta N + k_i \int \Delta N dt \tag{7}$$

where $\Delta N = N_{ord} - N_e$, N_{ord} is the engine ordered speed and N_e is the actual speed, k_i and k_p are the integral and proportional constant, and u_0 is the initial rack position.

2.2 Propeller modeling

The ship propeller is fixed pitch and its thrust and torque are determined using the dimensionless coefficients (K_T and K_Q) of thrust and torque, respectively, the sea water density (ρ_w), the propeller rotational speed (N_p(*rev/s*)) and the propeller diameter(D_p) [13,28]:

$$T_p = K_T \rho_w N_p^2 D_p^4 \beta \tag{8}$$

$$Q_p = K_Q \rho_w N_p^2 D_p^5 \beta^{0.8} \tag{9}$$

In calculating the amount of thrust and torque due to the emergence of propeller, the effect of free surface and the effect of Wagner should be considered. According to Faltinsen et al. [5] suggestion, the amount of thrust loss is proportional to the area of the propeller disc that is out of the water. When the propeller comes out of the water, after re-entering the water, it needs some time to be able to develop and recover its thrust, thus reducing the average amount of torque and thrust. According to Minsaas et al. [29] this parameter is also effective in the average amount of torque and thrust losses. When the ship's propeller is active near the surface of the water, it creates waves on the free surface, which also causes torque and thrust losses. The sum of these effects is formulated as follows by a thrust diminution factor (β) proposed by Minsaas et al. [29] and multiplied by the thrust and torque values.

$$\beta = \begin{cases} 1 - 0.675\left[1 - 0.769\left(\frac{h}{R}\right)\right]^{1.258} & \frac{h}{R} < 1.3 \\ 1 & \frac{h}{R} \geq 1.3 \end{cases} \tag{10}$$

where h is depth of the propeller shaft, R is propeller radius.

The dimensionless torque and thrust coefficients are determined from interpolating the polynomial equations for the Wageningen B-type propellers:

$$K_Q = \sum_{n=1}^{47} C Q_n J^s \left(\frac{P}{D}\right)^t \left(\frac{AE}{AO}\right)^u z_P^v \tag{11}$$

$$K_T = \sum_{n=1}^{39} CT_n J^s \left(\frac{P}{D}\right)^t \left(\frac{A_E}{A_O}\right)^u Z_P^v \tag{12}$$

where CQ_n and CT_n are the polynomial coefficients, A_E/A_O is the blade area ratio, P/D is the pitch to diameter ratio at 70% of the propeller radius for the fixed pitch propeller type, J is the propeller advance ratio, and Z_P is the number of propeller blades.

The propeller advance coefficient (J) depends on the propeller inflow velocity (V_{Total}), the propeller rotational speed (N_p (rps)) and the propeller diameter (D_p).

$$J = \frac{V_{Total}}{N_p D_p} \tag{13}$$

One of the influential factors in the dynamic analysis of the ship powertrain system is the information about wake in adverse weather conditions, which is very limited. Therefore, a correct estimate must be obtained from it. Research shows that the motion of a ship and the presence of waves will cause wake velocity fluctuations that have a mean value different from that of calm water [3]. The propeller average wake inflow velocity is affected by ship surge and pitch motions and the waves, which can be extracted according to the following equation [5,6]:

$$V_{Total} = \begin{pmatrix} (1-w_p)\{V_S - \omega_e \xi_a \sin(\omega_e t - \zeta_\xi)\} + \alpha\omega h_a \exp(-kz_p) \\ \cos X \cos(\omega_e t - kx_p \cos X) \end{pmatrix} \sqrt{\left(1 - \frac{\Delta\bar{p}}{0.5\rho V_S^2}\right)} \tag{14}$$

where

$$\Delta\bar{p} \sim -\frac{\rho}{4}\omega_e^2 |\eta_5|^2 x^2 \tag{15}$$

and w_p is effective wake fraction, V_S is ship speed, ω_e is wave encounter circular frequency, ξ_a is surge amplitude, ζ_ξ is phase delay, ω is wave circular frequency, h_a is wave amplitude, k is wave number, z_p is the immersion depth of the propeller shaft, x is the longitudinal distance of the propeller from the center of gravity of the ship, x_p is the position of the propeller section with reference to the center of gravity of the vessel, $\Delta\bar{p}$ is pressure gradient below the bottom of the ship due to pitching motion, X is wave encounter angle (0 for following sea; 180 for head sea), ρ is density of seawater, t is time, η_5 is pitch amplitude.

2.3 Ship dynamics modeling

In the process of ship modeling, only motion along its longitudinal axis is considered. Hence, the speed of the ship is determined by integrating the Eq. (16) which is expressed according to the dynamics of the ship:

$$\frac{dV_s}{dt} = \frac{(1-t\_d)T_p - (R_S + R_{Add})}{m_{ship} + m_{add}} \tag{16}$$

where V_s is the ship's longitudinal velocity, T_p is the effective propeller thrust, R_S is the ship's resistance which is calculated by the Holtrop [30] method in calm water conditions, t_d is the thrust deduction factor, m_{ship} is the ship's mass, m_{add} is the added virtual mass to consider the hydrodynamic force owing to the acceleration of a body in a fluid. R_{AW} is added resistance in wave and was calculated according to the following formula proposed by Liu et al [31]:

$$R_{AW} = R_{AWR} + R_{AWM} \tag{17}$$

The added resistance component (R_{AWR}) due to reflection/diffraction effect can be derived as:

$$R_{AWR} = \frac{2.25}{2}\rho g B \zeta_a^2 \alpha_T \sin^2 E \left(1+5\sqrt{\frac{L_{PP}}{\lambda}}Fn\right)\times\left(\frac{0.87}{C_B}\right)^{1+4\sqrt{Fn}} \tag{18}$$

where

$$\alpha_T = \begin{cases} 1-e^{-4\pi\left(\frac{T}{\lambda}-\frac{T}{2.5L_{PP}}\right)} & \lambda/L_{PP} \le 2.5 \\ 0 & \lambda/L_{PP} > 2.5 \end{cases}$$

E(=arctan(B/(2L_E)) as shown in Fig. 1 and R_{AWM} are the angle of entrance of waterline and the component of the added resistance due to motion/radiation effect, respectively. B and L_E are ship'sbeam and length of waterline entrance, respectively. L_{PP} is length of ship between perpendiculars, ζ_a is incident wave amplitude, λ is wave length, ρ is seawater density, Fn is Froude number and g is gravitational acceleration.

$$R_{AWM} = 4\rho g \zeta_a^2 B^2 / L_{PP} \bar{\omega}^{b1} \exp\left[\frac{b_1}{d_1}(1-\bar{\omega}^{d1})\right] a_1 a_2 a_3 \tag{19}$$

where

$$a_1 = 60.3 C_B^{1.34} (4k_{yy})^2 \left(\frac{0.87}{C_B}\right)^{(1+Fn)} \left(\ln\frac{B}{T}\right)^{-1}$$

$$a_2 = \begin{cases} 0.0072 + 0.1676Fn & Fn \prec 0.12 \\ Fn^{1.5}\exp(-3.5Fn) & Fn \ge 0.12 \end{cases}$$

$$a_3 = 1.0 + 0.25 \arctan\frac{\delta T}{L_{PP}}$$

and C_B is ship's block coefficient, k_{yy} is non-dimensional longitudinal mass radius of gyration (pitch), as percentage of L_{PP}, T is draft of the ship and δT is the draft difference between the fore perpendicular and aft perpendicular, and the unit of arctan ($\delta T / L_{PP}$) is in degree.

$$\bar{\omega} = \begin{cases} 2.142\sqrt[3]{k_{yy}}\sqrt{\frac{L_{PP}}{\lambda}}\left[1-0.13\frac{0.85}{C_B}\left(\ln\frac{B}{T}-\ln 2.75\right)\right](Fn+0.62) & Fn<0.10 \\ 2.142\sqrt[3]{k_{yy}}\sqrt{\frac{L_{PP}}{\lambda}}\left[1-0.13\frac{0.85}{C_B}\left(\ln\frac{B}{T}-\ln 2.75\right)\right]Fn^{0.143} & Fn\ge 0.10 \end{cases}$$

For $C_B \le$ 0.75

$$b_1 = \begin{cases} 11.0 & \bar{\omega} < 1 \\ -8.5 & \bar{\omega} \ge 1 \end{cases}$$

$$d_1 = \begin{cases} 14.0 & \bar{\omega} < 1 \\ -566\left(\frac{L_{PP}}{B}\right)^{-2.66} \times 6 & \bar{\omega} \ge 1 \end{cases}$$

and for $C_B >$ 0.75

$$b_1 = \begin{cases} 11.0 & \bar{\omega} < 1 \\ -8.5 & \bar{\omega} \ge 1 \end{cases}$$

$$d_1 = \begin{cases} -566\left(\frac{L_{PP}}{B}\right)^{-2.66} & \bar{\omega} < 1 \\ -566\left(\frac{L_{PP}}{B}\right)^{-2.66} \times 6 & \bar{\omega} \geq 1 \end{cases}$$

The added resistance due to wind can be derived using [33]:

$$R_{AA} = \frac{1}{2}\rho_A V_{WR}^2 C_X(\psi_{WR}) A_{XV} \tag{20}$$

where ρ_A denotes air mass density, V_{WR} is relative wind speed, $C_X(\psi_{WR})$ is wind resistance coefficient, A_{XV} is area of maximum transverse section exposed to the wind and ψ_{WR} denotes relative wind direction. Therefore, the total resistance due to the weather conditions can be estimated as follows:

$$R_{TWC} = R_{AW} + R_{AA} \tag{21}$$

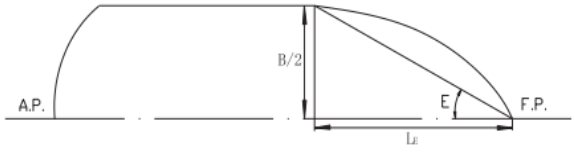

Fig.1
Definition of length L_E and angle E of entrance of waterline [32].

2.4 Validation

The propulsion system of a VLCC is simulated in Simulink based on the principles, developed and verified formulations. The ship, engine, propeller and shafting system specifications are shown in Table 1. For simulation, various data including engine, ship, propeller and work space (air, exhaust gases, seawater, etc.) specifications were used. To simulate, the multi-input multi-output (MIMO) modeling system is used in which the required speed of the ship or the engine ordered speed (set-point speed) and the number of active cylinders are assumed as inputs and the performance parameters of the engine and ship such as engine torque, speed, fuel consumption, emissions, ship propeller thrust, ship speed and etc. are considered as model outputs as can be seen in the Fig. 2. To validate the developed model, fuel consumption measurement report [36] for a VLCC related to a 12-day voyage cycle in calm water as shown in Fig. 3 was used. In this report, the daily fuel consumption of this ship for a period of twelve days at sea is shown. The fuel consumption results predicted by developed model and similar respective values from the VLCC report are shown in Fig. 3, which highlights and validates the accuracy of the developed model.

The difference between the predicted values, 49.91 Tons/day and 598.98 Tons for Average daily fuel consumption and total consumption, respectively, of the present model and VLCC fuel consumption measurement report, 51.65 Tons/day and 619.85 Tons for average daily fuel consumption and total consumption, respectively, is approximately 3.5% for the same voyage cycle of VLCC.

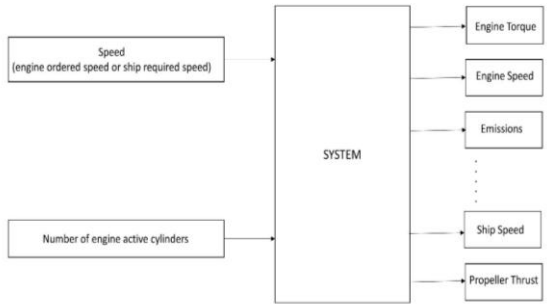

Fig.2
Schematic of the VLCC ship system as a multi-input multi-output system.

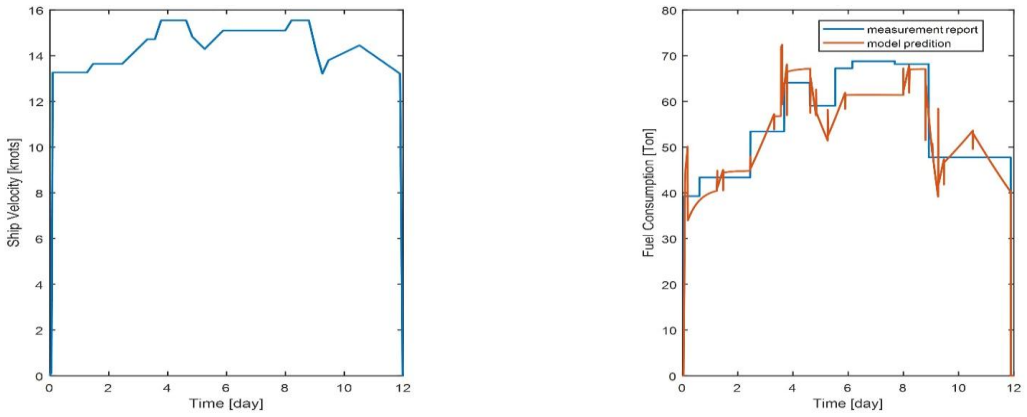

(a) (b)

Fig.3
(a) VLCC ship voyage cycle; (b) fuel consumption.

Table 1
VLCC ship powertrain specifications [34,35].

Engine			Intermediate shaft		
Type	7RT-flex82T	2-stroke	Diameter	d_1	0.7 [m]
Cylinder no.	7	In-line	Length	l_1	9.927 [m]
Output (CMCR)	31640 [Kw]		Inertia		1376 [kgm^2]
Propeller			Ultimate-tensile strength	UTS	590 [N/mm^2]
Blades no.		4	Yield stress		295[N/mm^2]
Diameter	d_p	9.86 [m]	Shear modulus	G_1	81.4 [GPa]
Damping (CMCR)	B_p	467580 [Nms/rad]	Density	ρ_1	7850 [kg/m^3]
Load inertia	J_p	429250 [kgm^2]	Propeller shaft		
Flywheel			Diameter	d_2	0.85 [m]
Inertia	J_f	13600 [kgm^2]	Length	l_2	10.233 [m]
Damping (CMCR)	B_f	9115 [Nms/rad]	Inertia		3454 [kgm^2]
Ship			Ultimate tensile strength	UTS	590 [N/mm^2]
Length	L	320 [m]	Yield stress		295[$N/mm2$]
Breadth	B	58 [m]	Shear modulus	G_2	81.4 [GPa]
Displacement volume	V	312622 [m^3]	Density	ρ_2	7850 [kg/m^3]
Area of maximum transverse section exposed to the wind	A_{XV}	1161[m^2]			

3 POWERTRAIN SYSTEM MODEL

The physical system modeling is modified to achieve a better prediction of its performance. The model should have adequate matching with the system so that reasonably well represents the characteristics of the real physical system. Fig. 4 shows a schematic layout of a VLCC ship powertrain system under consideration. The finite element and hybrid distributed-lumped modelling techniques are considered for dynamic analysis of the system.

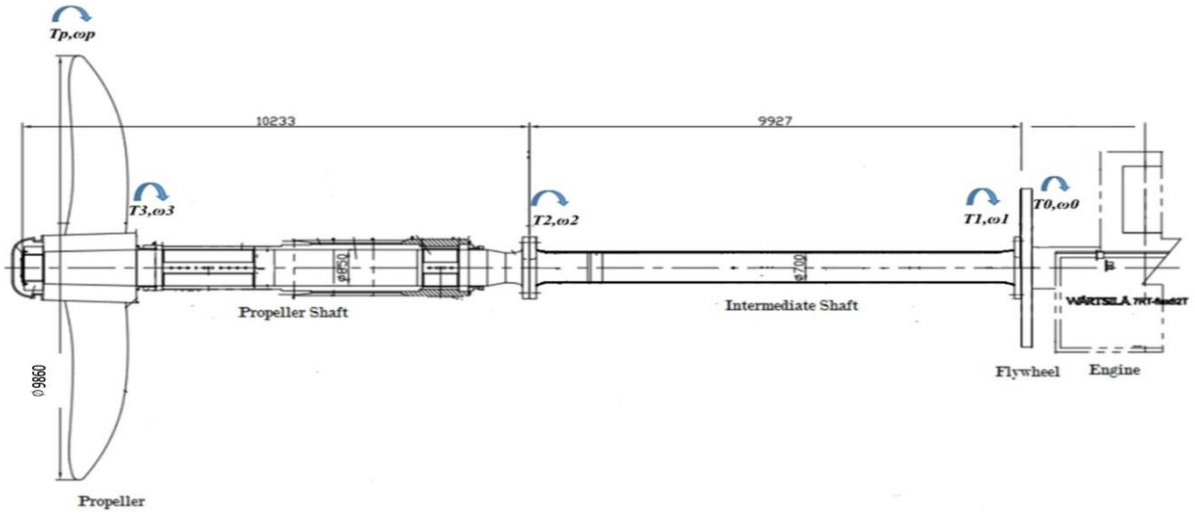

Fig.4
Schematic layout of VLCC ship powertrain system [34].

3.1 Finite element model

Finite element method is one of the most widely used methods for analyzing engineering problems. In fact, the finite element method is a numerical method for solving partial differential equations in which a system is subdivided into smaller and simpler parts called finite elements. In this section, the intermediate shaft and propeller shaft are divided into ten similar sections, where governing equations for each sections are presented by Eqs. (22).

$$\begin{aligned}
&T_0(t) = J_f D^2\theta_0(t) + D_f D\theta_0(t) + k_1(\theta_0(t) - \overline{\theta_1}(t));\\
&0 = \overline{J}_1 D^2\overline{\theta_1}(t) - k_1(\theta_0(t) - \overline{\theta_1}(t)) + k_2(\overline{\theta_1}(t) - \overline{\theta_2}(t));\\
&\vdots\\
&0 = \overline{J_{19}} D^2\overline{\theta_{19}}(t) - k_{19}(\overline{\theta_{18}}(t) - \overline{\theta_{19}}(t)) + k_{20}(\overline{\theta_{19}}(t) - \overline{\theta_p}(t));\\
&0 = J_p D^2\theta_p(t) + D_p D\theta_p(t) + k_{20}(\theta_p(t) - \overline{\theta_{19}}(t));
\end{aligned} \tag{22}$$

where $\overline{J_{10}} = 0;\ D\overline{\theta_j}(t) = \overline{\omega_j}(t), 1 \le j \le 19;$ and $D\theta_k(t) = \omega_k(t), k = 0, p;$ Eqs. (22) with zero initial conditions using Laplace transformation is:

$$\begin{bmatrix} T_0(s) \\ 0 \\ 0 \\ \vdots \\ 0 \end{bmatrix}_{21\times1} = [Js^2 + Cs + K] \begin{bmatrix} \theta_0(s) \\ \overline{\theta_1}(s) \\ \vdots \\ \overline{\theta_{19}}(s) \\ \theta_p(s) \end{bmatrix}_{21\times1} \tag{23}$$

where $J_{(21\times21)} = diag(J_f, \overline{J_1}, ..., \overline{J_{19}}, J_p);\quad C_{(21\times21)} = diag(D_f, 0, ..., 0, D_p);\quad K = \begin{bmatrix} k_1 & -k_1 & 0 & 0 & \cdots & 0 \\ -k_1 & k_1+k_2 & -k_2 & 0 & \cdots & 0 \\ 0 & -k_2 & k_2+k_3 & -k_3 & \cdots & 0 \\ 0 & 0 & & & & \vdots \\ \vdots & \vdots & & & & -k_{20} \\ 0 & 0 & \cdots & 0 & -k_{20} & k_{20} \end{bmatrix}_{21\times21}$

Assuming that all intermediate shaft segments are parallel with same length and diameter, thus: $\overline{J}_1 = \overline{J}_2 = \ldots = \overline{J}_9 = \hat{J}$; and

$$k_1 = k_2 = \cdots = k_{10} = \hat{k}; \tag{24}$$

with similar logic for propeller shaft: $\overline{J}_{11} = \overline{J}_{12} = \ldots = \overline{J}_{19} = \hat{J}$; and

$$k_{11} = k_{12} = \ldots = k_{20} = \hat{k}; \tag{25}$$

Consequently, the angular speeds can be determined by:

$$\begin{bmatrix} \omega_0(s) \\ \overline{\omega_1}(s) \\ \vdots \\ \overline{\omega_{19}}(s) \\ \omega_p(s) \end{bmatrix}_{21\times 1} = s[Js^2 + Cs + K]^{-1} \begin{bmatrix} T_0(s) \\ 0 \\ 0 \\ \vdots \\ 0 \end{bmatrix}_{21\times 1} \tag{26}$$

Substituting $s=i\omega$ in $\frac{\det[Js^2 + Cs + K]}{s}$ and by equating the imaginary part of this expression to zero, the resonant frequencies of this finite element model can be determined. Calculations show that for this model, each of the shafts is divided into ten equal parts, the number of eigenvalues produced is thirty-nine while the lumped parameter model generates three eigenvalues. Increasing the number of shaft sections in the finite element model would increase computational cost, time and possibly errors.

3.2 Distributed-Lumped model

In distributed modeling as an analytical method, fundamental assumption is that the dynamic system comprises an infinite number of elements that are infinitesimal. Hybrid (Distributed-Lumped) model is a combination of lumped and distributed models of assemblies that exist in the dynamic systems. The modeling and simulation of hybrid systems such as long geared drive shafts and loads, the flow of air/gas through long tunnels or ducts and large structures have been studied by Whalley [37]. Hybrid systems can be structured as a series of distributed-lumped sections in the form of a system impedance matrix or a system admittance matrix, as presented by other researchers [38]. Gholami et al. [39] used the distributed-lumped modeling method to calculate dynamic shear stresses for different diameters of propeller shaft of a merchant ship over a range of operational speed. The results showed that improving propeller shaft design could reduce significantly the shaft mass and material saved specially at slow steaming is much greater than normal speeding case.

3.2.1 Distributed shafts

In this method, the lumped parts of the powertrain system are assumed to be flywheel and propeller. The intermediate shaft and propeller shaft are the distributed components of ship powertrain system. Using Newton's second law, the governing equations for a distributed shaft of length Δx, as shown in Fig. 5 can be expressed as follows where, $\theta(x,t)$ and $T(x,t)$ are angle of twist and twisting moment, respectively.

$$T(x,t) = -GJ \frac{\partial \theta(x,t)}{\partial x} \tag{27}$$

and differentiating with respect to time (t);

$$\frac{\partial \omega(x,t)}{\partial x} = -C\,\frac{\partial T(x,t)}{\partial t}; \tag{28}$$

and

$$[T(x,t)+\Delta T(x,t)]-T(x,t) = -J\rho\frac{\partial^2\theta(x,t)}{\partial^2 t}\Delta x \tag{29}$$

then

$$\frac{\partial T(x,t)}{\partial x} = -L\,\frac{\partial \omega(x,t)}{\partial t} \tag{30}$$

where

$$\omega(x,t) = \frac{\partial\theta(x,t)}{\partial t}; \qquad \Delta T(x,t) = \frac{\partial T(x,t)}{\partial x}\Delta x; \qquad L = J\rho; \qquad C = \frac{1}{GJ};$$

Therefore

$$\frac{\partial T(x,t)}{\partial x} = -J_{sj}\,\rho_j\,\frac{\partial \omega(x,t)}{\partial t} \tag{31}$$

$$\frac{\partial \omega(x,t)}{\partial x} = -\frac{1}{G_j J_{sj}}\frac{\partial T(x,t)}{\partial t} \tag{32}$$

where x is distance from end of the shaft and T and ω are torque and angular velocity, respectively. J_{sj} is polar moment of inertia of the shaft (m^4), ρ_j is the shaft density (kg/m^3). G_j and t are shear modulus of rigidity of the shaft and time, respectively. C and L are shaft's compliance and inertia per unit length, respectively. Using Eqs. (31) and (32) in z domain for the two distributed shafts shown in Fig. 4, the relationship between the angular velocity and the applied torque in finite delay form can be expressed as:

$$\begin{bmatrix}\omega_1\left(z_1^{-1}\right)\\ \omega_2\left(z_1^{-1}\right)\end{bmatrix} = 1/\xi_1 \times \begin{bmatrix}\dfrac{1+z_1^{-1}}{1-z_1^{-1}} & -2\dfrac{z_1^{-\frac{1}{2}}}{1-z_1^{-1}}\\ 2\dfrac{z_1^{-\frac{1}{2}}}{1-z_1^{-1}} & -\dfrac{1+z_1^{-1}}{1-z_1^{-1}}\end{bmatrix}\begin{bmatrix}T_1\left(z_1^{-1}\right)\\ T_2\left(z_1^{-1}\right)\end{bmatrix} \tag{33}$$

For the intermediate shaft (admittance module), and

$$\begin{bmatrix}T_2(z)\\ T_3(z)\end{bmatrix} = \xi_2\begin{bmatrix}\dfrac{1+z_2^{-1}}{1-z_2^{-1}} & -2\dfrac{z_2^{-\frac{1}{2}}}{1-z_2^{-1}}\\ 2\dfrac{z_2^{-\frac{1}{2}}}{1-z_2^{-1}} & -\dfrac{1+z_2^{-1}}{1-z_2^{-1}}\end{bmatrix}\begin{bmatrix}\omega_2\left(z_2^{-1}\right)\\ \omega_3\left(z_2^{-1}\right)\end{bmatrix} \tag{34}$$

For the propeller shaft (impedance module), where

$$z_1^{-1} = \mathrm{e}^{\left(-2l_1\sqrt{L_1C_1}\right)s} \tag{35}$$

$$z_2^{-1} = e^{\left(-2l_2\sqrt{L_2C_2}\right)s} \tag{36}$$

and

$$\xi_1 = \sqrt{\frac{L_1}{C_1}} \tag{37}$$

$$\xi_2 = \sqrt{\frac{L_2}{C_2}} \tag{38}$$

The finite time delays and characteristic impedances respectively,

$$C_j = \frac{1}{G_j J_{sj}} \qquad L_j = J_{sj}\rho_j \qquad j = 1,2 \tag{39}$$

The dynamic shear stress for the intermediate and propeller shafts can be calculated using the following formula:

$$\tau_j(s) = \frac{0.5G_j d_j}{l_j}\left(\frac{\omega_i - \omega_{i+1}}{s}\right) \qquad i = 0,1,2; \tag{40}$$

In finite delay form, it can be expressed as:

$$\tau_j(z_j^{-1}) = \frac{0.5G_j d_j}{l_j}\left(\frac{\omega_i - \omega_{i+1}}{1 - z_j^{-1}}\right) \tag{41}$$

ω_i and ω_{i+1} are angular speeds of shafts.

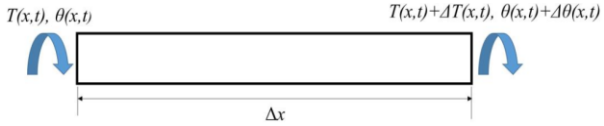

Fig.5
A shaft in torsion.

3.2.2 Lumped flywheel model

The governing equation for the lumped flywheel using Laplace transformation with zero initial condition is,

$$T_f(s) = (J_f s + B_f)\omega_f(s) \tag{42}$$

Transforming Eq. (42) to the z domain yields

$$\frac{\omega_f}{T_f}(z_1) = \frac{\beta_f z_1}{z_1 + \alpha_f} \tag{43}$$

where

$$\beta_f = \frac{1-\alpha_f}{B_f} \tag{44}$$

$$\alpha_f = \exp\left(-\frac{B_f}{J_f} 2l_1 \sqrt{L_1 C_1}\right) = \exp\left(-\frac{B_f}{J_f} 2l_1 \sqrt{\rho_1 / G_1}\right) \tag{45}$$

In finite delay form, Eq. (43) becomes

$$T_f\left(z_1^{-1}\right) = \frac{1-\alpha_f z_1^{-1}}{\beta_f} \omega_f\left(z_1^{-1}\right) \tag{46}$$

3.2.3 Lumped propeller model

The governing equation for the lumped propeller using Laplace transformation with zero initial conditions is,

$$T_p(s) = \left(J_p s + B_p\right) \omega_p(s) \tag{47}$$

After transforming Eq. (47) to z domain,

$$\frac{\omega_p}{T_p}(z_2) = \frac{\beta_p z_2}{z_2 + \alpha_p} \tag{48}$$

where

$$\alpha_p = \exp\left(-\frac{B_p}{J_p} 2l_2 \sqrt{L_2 C_2}\right) = \exp\left(-\frac{B_p}{J_p} 2l_2 \sqrt{\rho_2 / G_2}\right) \tag{49}$$

In finite delay form,

$$\omega_p\left(z_2^{-1}\right) = \frac{\beta_p}{1-\alpha_p z_2^{-1}} T_p\left(z_2^{-1}\right) \tag{50}$$

In this stage, the distributed-lumped model used in the present study was validated with respect to a marine transmission system distributed model presented by Bartlett et al. [39]. As shown in Fig. 6, the results are in a good agreement with Bartlett et al. modeling results. In the second stage, the distributed-lumped model was used to simulate the dynamical behavior of the ship powertrain system.

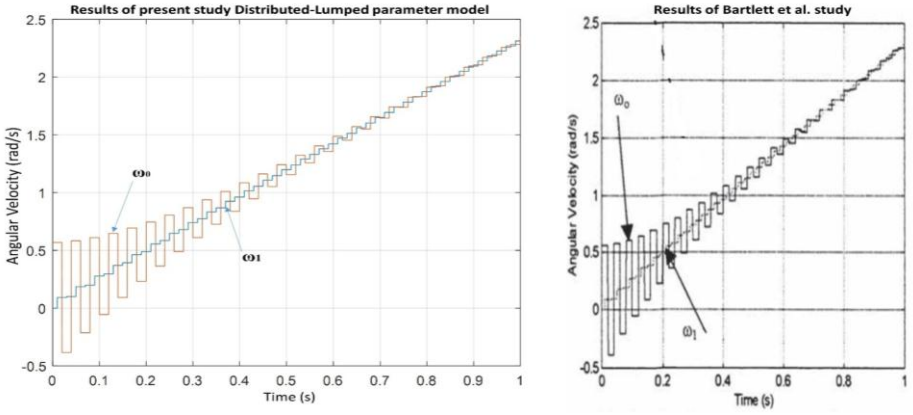

Fig.6
Assessment of Bartlett et al. study and present study using Distributed-Lumped model for a ship powertrain system.

4 RESULTS AND DISCUSSION

In this section, the effects of using different modeling methods mentioned in the previous sections in predicting the dynamic behavior of the system in the face of adverse weather conditions have been investigated. In all these models, the weather is assumed to be violent storm in head waves with a wave height of 11.5 *m* and wind speed of 28.5 *m/s* in accordance with ITTC 2017 [40] guidelines for preparation, conduct and analysis of speed/power trials. The wavelength to the length of ship between perpendicular ratio (λ/L_{PP}) for these scenarios will be 1. In this section the behavior of the ship system is investigated and it is assumed that the ship is in full load condition. In order to simulate the system, the engine speed change was considered as input to the system in the form of a step signal. It is assumed that the initial value is 45 *rpm* for different simulation modes and at time of 2 *s*, this value changes to 80 *rpm* abruptly. It is also assumed that all engine cylinders (seven cylinders) are active. Then the amounts of the performance parameters such as speed and torsional shear stress for different modes are calculated and plotted. The results were extracted after simulation for a period of 1.0 seconds.

4.1 Comparison of the methods

In the first stage, it is assumed that the shafting system is a rigid body and since the mass moments of inertia of the intermediate shaft and propeller shaft are small compared to the mass moments of inertia of engine and propeller of the ship, therefore the mass moment of inertia values of these shafts are added to the mass moments of inertia of the engine and propeller. On the other hand, due to the high power generation of the propulsion system, the damping values and energy losses in the drive-train system are considered to be negligible.

In the second stage, unlike the first stage, the intermediate shaft and propeller shaft are dynamically modelled using finite element method and distributed-lumped method and the results of these methods are compared with the results of other techniques such as lumped parameter method. Predicted results from various modeling techniques to investigate the dynamic behavior of the ship powertrain system are shown in Figs. 7 to 12.

The results presented in the Figs. 7 to 12 indicates that there are clear differences between the responses obtained from the rigid model and the responses of other models. In the rigid model, assuming that the mass moments of inertia of the entire powertrain system, including the transmission shafts, engine and propeller of the ship, are aggregated together and assumed as an independent body, therefore the oscillations observed in other models, not seen in the rigid model.

As shown in Figs. 9 to 12, the predicted results of the system speed and torque as well as the calculated dynamic shear stress in the transmission shafts are similar to each other. The similarity of the obtained responses can be due to the high amount of inertia and damping, low stiffness, slenderness ratio and system dispersion. At first glance, it seems that using any of the proposed models for dynamic analysis of this system can be appropriate and accurate enough, but what is discussed here is whether all the models presented, in terms of calculations such as time which are needed to run the model, are suitable, or if used in redesigning the system, have sufficient accuracy. Although the lamped parameter technique is the simplest method of modeling, as the dispersion of the system expands, the accuracy of the responses resulting from the use of this method is greatly reduced. Therefore, the finite element method is used as a more accurate alternative to the lamped parameter method for the analysis of dynamic systems. Due to the fact that by increasing the number of elements assumed in the finite element method, the number of dynamic equations governing the system will also increase, hence the probability of computational error will increase. Due to the matrix operations and the processes of generating eigenvalues and eigenvectors in the finite element method, when the system has low inertia and damping or high stiffness, these can reduce the accuracy of calculations, increase the complexity of system analysis and create instability in the system response [41,42]. On the other hand, considering all the components of the system continuously will increase the complexity of the system and make it more difficult to analyze its dynamic behavior. In this paper, which uses different modeling methods to investigate the dynamic behavior of the VLCC powertrain system in the rough sea, the time consumed to run each of these models is presented in the Table 2.

Table 2
Run time for different methods.

Method	Rigid body	Lumped parameter	FE(5 sections)	FE(10 sections)	Hybrid(distributed-lumped)
Run time (seconds)	101	421	21386	57751	419

Interestingly, the implementation of the hybrid (distributed-lumped) method, in which it is assumed that the existing continuous systems, the power transmission shafts from the engine to the ship propeller, are composed of an infinite number of infinitesimal elements have a very short computational time that is comparable with the lamped method, which is the simplest method of modeling in this research. However, as can be seen in the finite element method, the computation time is greatly increased and reaches several hours, but the results show that there is no significant difference between the finite element method and the hybrid technique in terms of computational accuracy. Therefore, it seems that using a combination of lamped parameter and distributed methods can be the most appropriate method to analyze the behavior of the dynamic system.

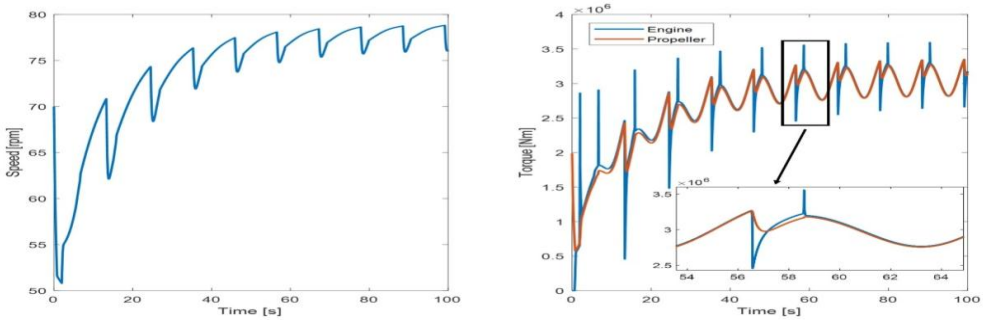

Fig.7
Engine speed and torque, assuming the shafting system as a rigid body.

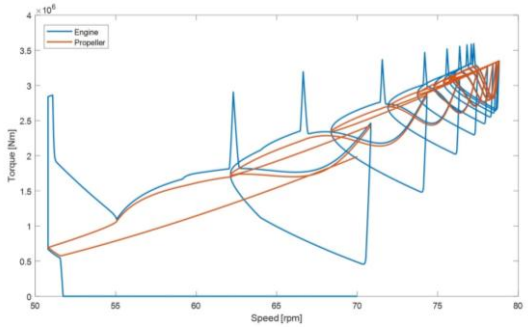

Fig.8
Engine torque vs. speed, assuming the shafting system as a rigid body.

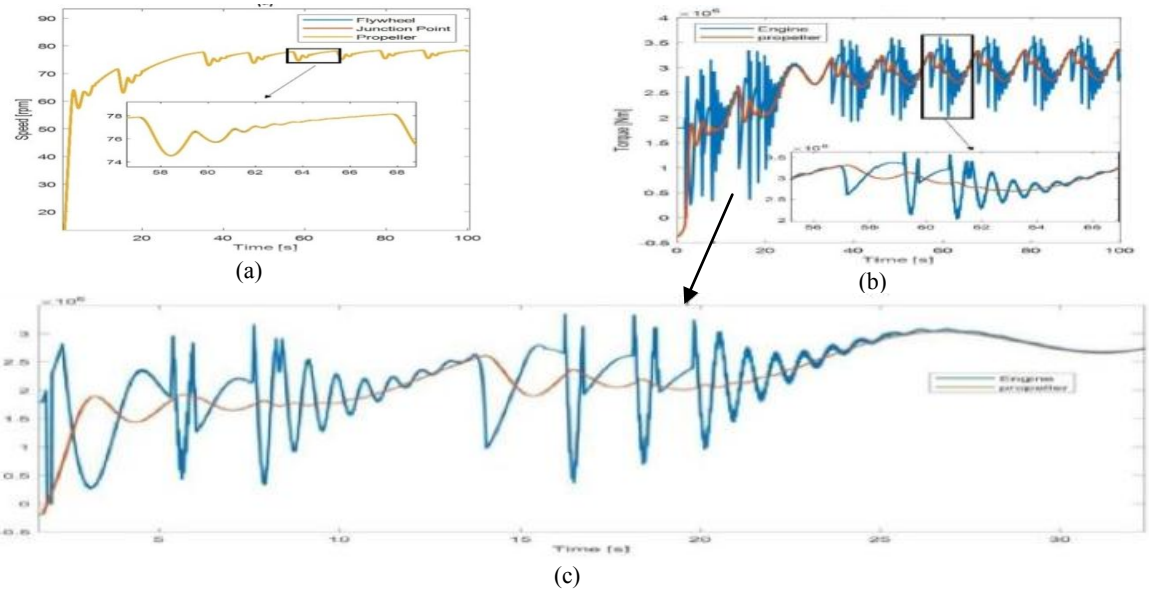

Fig.9
Engine speed and torque, each of intermediate & propeller shafts is divided into 10 similar sections according to the finite element method.

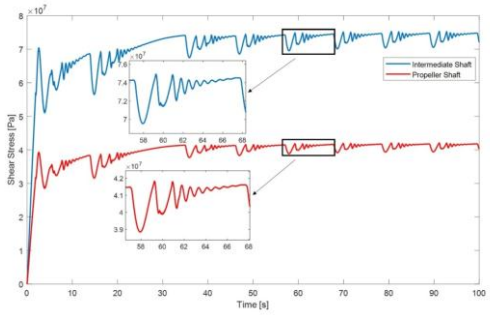

Fig.10
Shear stress of intermediate & propeller shafts, each of them is divided into 10 similar sections according to the finite element method.

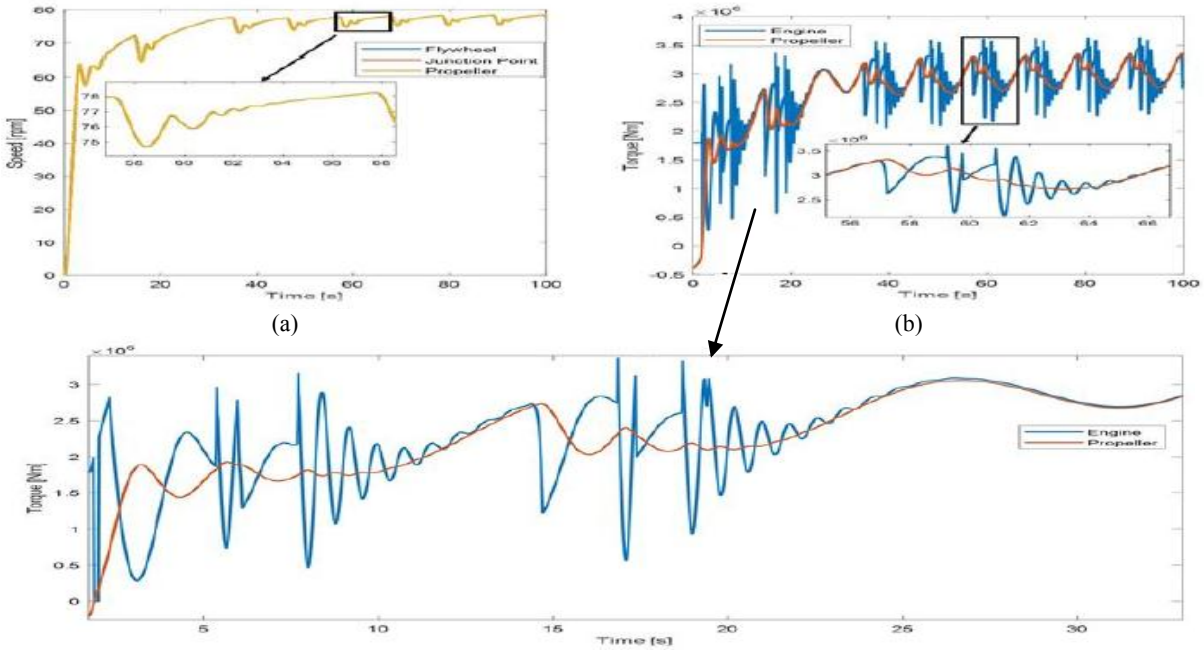

(a) (b)

(c)

Fig.11
Engine speed and torque for Hybrid (Distributed-Lumped) model.

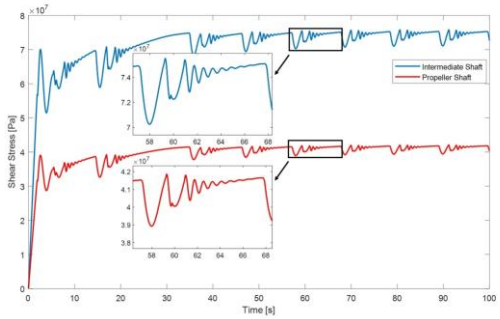

Fig.12
Shear stress of intermediate & propeller shafts for Hybrid (Distributed-Lumped) model.

4.2 Shafting system fatigue analysis

Fatigue life assessment is very important in ship powertrain systems. Fatigue analysis of power transmission shafts as components of power transmission from the engine to the ship and on the other hand as a system of transmitting forces from the seawater on the propeller to the engine is of great importance. Different loads such as low cycle, high cycle and transient can be applied to these shafts and may cause system fatigue and even failure. In this

research, using the values of shear stresses estimated in the previous sections, the fatigue analysis of the transmission shafts has been done according to the DNVGL guideline [43];

$$\tau_{vT} \le \tau_{vHC}\left(\frac{3\times10^{6}}{N_c}\right)^{0.4\log\left(\frac{\tau_{vLC}}{\tau_{vHC}}\right)} = \tau_{vLC}\left(\frac{N_c}{10^{4}}\right)^{0.4\log\left(\frac{\tau_{vHC}}{\tau_{vLC}}\right)} \tag{51}$$

where τ_{vHC} and τ_{vLC} are the permissible high and low cycle torsional vibration stress amplitudes, respectively, N_c is the accumulated number of load cycles and τ_{vT} is Permissible torsional vibration stress amplitude for transient condition. The permissible torsional vibration stress amplitude for transient condition is assumed to be equal to the maximum shear stresses calculated in the previous section for the intermediate and propeller shafts. Using the Eq. (51), the number of load cycles for the intermediate and propeller shafts will be 376 and 7.8×10^{8} cycles, respectively. In addition, the permissible vibration stresses in high cycle, low cycle and transient conditions, if the number of load cycles is assumed to be equal to 10^{5} cycles, are calculated as functions of engine speed for transmission shafts and can be seen in Fig. 13. Calculations show that considering the fatigue life of power transmission shafts, especially the intermediate shaft in the design stage will be of great importance and can not be ignored.

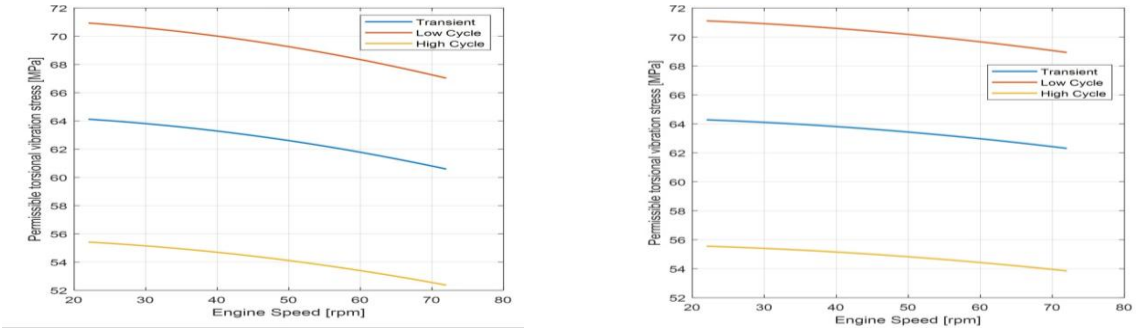

Fig.13
Permissible torsional vibration stress for: (a) intermediate shaft (b) propeller shaft.

5 CONCLUSION

In this study, the powertrain system of a VLCC (Very Large Crude oil Carrier) was analyzed using different method such as lumped parameter method, finite element method and distributed-lumped method. The effects of sea wave and wind on the engine and power transmission shafts were investigated. To validate the model, a fuel consumption report related to a 12-day voyage was taken into consideration. Comparison of the results of the modeling and the report indicates good agreement. In the next step, the effect of using different modeling methods for analysis of the intermediate shaft and propeller shaft was investigated and the system responses to these models were illustrated. Given that in distributed modeling as an analytical method, the basic assumption is that the dynamic system contains an infinite number of infinitesimally small elements, so the results of this modeling method can be more reliable than other modeling methods. Therefore, Hybrid (distributed-lumped) modeling method as an accurate and efficient modeling technique that requires little time to run the model can be used in the fatigue analysis and design of dynamic systems such as powertrain systems as expressed in this research.

REFERENCES

[1] IMO., 2011, *Air Pollution and Energy Efficiency-Estimated CO2 Emissions Reduction From Introduction of Mandatory Technical and Operational Energy Efficiency Measures for Ships*, International Maritime Organization, London.

[2] IMO., 2018, *Initial IMO GHG Strategy*, International Maritime Organization, London.

[3] Nakamura S., Naito S., 1975, Propulsive performance of a container ship in waves, *Journal of the Society of Naval Architects of Japan* **15**: 24-48.

[4] Amini H., 2011, Azimuth propulsors in off-design conditions, *NTNU* **186**: 1503.

[5] Faltinsen O.M., Minsaas K.J., Liapis N., Skjordal S.O., 1980, Prediction of resistance and propulsion of a ship in a seaway, *Proceedings of the 13th Symposium on Naval Hydrodynamics*.

[6] Ueno M., Tsukada Y., Tanizawa K., 2013, Estimation and prediction of effective inflow velocity to propeller in waves, *Journal of Marine Science and Technology* **18**(3): 339-348.

[7] Guo B.J., Steen S., Deng G.B., 2012, Seakeeping prediction of KVLCC2 in head waves with RANS, *Apple Ocean Research* **35**(0): 56-67.

[8] Taskar B., Yum K.K., Steen S., Pedersen E., 2016, The effect of waves on engine-propeller dynamics and propulsion performance of ships, *Ocean Engineering* **122**: 262-277.

[9] Kayano J., Yabuki H., Sasaki N., Hiwatashi R., 2013, A study on the propulsion performance in the actual sea by means of full-scale experiments, *TransNav, The International Journal on Marine Navigation and Safety of Sea Transportation* **7**(4): 521-526.

[10] Larroude V., Chenouard R., Yvars P.A., Millet D., 2013, Constraint based approach for the steady-state simulation of complex systems: Application to ship control, *Engineering Applications of Artificial Intelligence* **26**: 499-514.

[11] Kyrtatos N.P., Theodossopoulos P., Theotokatos G., Xiros N., 1999, Simulation of the overall ship propulsion plant for performance prediction and control, *Proceedings of the Conference on Advanced Marine Machinery Systems with Low Pollution and High Efficiency.*

[12] Scappin F., Stefansson S.H., Haglind F., Andreasen A., Larsen U., 2012, Validation of a zero- dimensional model for prediction of NOx and engine performance for electronically controlled marine two stroke diesel engines, *Applied Thermal Engineering* **37**: 344-352.

[13] Yum K.K., Taskar B., Pedersen E., Steen S., 2017, Simulation of a two-stroke diesel engine for propulsion in waves, *International Journal of Naval Architecture and Ocean Engineering* **9**(4): 351-372.

[14] Bazari Z., 1994, Diesel Exhaust Emissions Prediction under Transient Operating Conditions, *International Congress & Exposition* **103**: 940666.

[15] Theotokatos G., Tzelepis V., 2015, A computational study on the performance and emission parameters mapping of a ship propulsion system, *Proceedings of the Institution of Mechanical Engineers, Part M : Journal of Engineering for the Maritime Environment* **229**: 58-76.

[16] Rao S.S., 2010, *Mechanical Vibrations*, Pearson Education, Inc., Publishing as Prentice Hall.

[17] Nelson H.D., McVaugh J.M., 1976, The dynamics of rotor-bearing systems using finite elements, *Journal of Engineering for Industry* **98**: 593-600.

[18] Murawski L., Charchalis A., 2014, Simplified method of torsional vibration calculation of marine power transmission system, *Marine Structures* **39**: 335-349.

[19] Chahr-Eddine K., Yassine A., 2014, Forced axial and torsional vibrations of a shaft line using the transfer matrix method related to solution coefficients, *Journal of Marine Science and Application* **13**: 200-205.

[20] Huang Q., Zhang C., Jin Y., Yuan C., Yan X., 2015, Vibration analysis of marine propulsion shafting by the coupled finite element method, *Journal of Vibroengineering* **17**: 3392-3403.

[21] Jang M.O., Kim U.K., Park Y.N., Lee Y.J., 2004, A study on the coupled torsional-axial vibration of marine propulsion shafting system using the energy method, *Journal of the Korean Society for Marine Environment & Energy* **28**: 482-492.

[22] Yang Y., Che C., Tang W., 2014, Shafting coupled vibration research based on wave approach, *Journal of Shanghai Jiaotong University (Science)* **19**: 325-336.

[23] Huang Q., Liu H., Cao J., 2019, Investigation of lumped-mass method on coupled torsional-longitudinal vibrations for a marine propulsion shaft with impact factors, *Journal of Marine Science and Engineering* **7**: 95.

[24] Grzadziela A., 2008, Modelling of propeller shaft dynamics at pulse load, *Polish Maritime Research* **15**(4): 52-58.

[25] Kluczyk M., Grzadziela A., 2017,Vibration diagnostics of the naval propulsion systems, *Scientific Journal of Polish Naval Academy* **1**(208): 15-29.

[26] Xiros N., 2002, *Robust Control of Diesel Ship Propulsion*, Springer.

[27] Heywood J.B., 1988, *Internal Combustion Engines Fundamentals*, McGraw-Hill, New York.

[28] Carlton J.S., 2007, *Marine Propellers and Propulsion*, Butterworth-Heinemann, Oxford, UK.

[29] Minsaas K., Faltinsen O.M., Persson B., 1983, On the importance of added resistance, propeller immersion and propeller ventilation for large ships in a seaway, *Proceedings of the 2nd International Symposium on Practical Design in Shipbuilding*, Tokyo & Seoul.

[30] Holtrop J., Mennen G., 1982, An approximate power prediction method, *International Shipbuilding Progress* **329**: 166-170.

[31] Liu S., Shang B., Papanikolaou A., 2019, On the resistance and speed loss of full type ships in a seaway, *Ship Technology research (Schiffstechnik)* **66**(3): 163-181.

[32] Liu S., Papanikolaou A., 2017, Approximation of the added resistance of ships with small draft or in Ballast condition by empirical formula, *Proceedings of the Institution of Mechanical Engineers - Part M, Journal of Engineering for the Maritime Environment* **231**: 1-14.

[33] International Towing Tank Conference-Recommended Procedures and Guidelines, Analysis of Speed/Power Trial Data, 7.5-04-01-01.2, Effective Date 2014, Revision 01.
[34] Dalian Shipbuilding Industry Co.,Ltd (DSIC), QMD Technical Analysis & Support, Torsional Vibration Calculation, Calculation No. : DTA-TV-C-R-0014b.
[35] Yasukawa H., Zaky M., Yonemasu I., Miyake R., 2017, Effect of engine output on maneuverability of a VLCC in still water and adverse weather conditions, *Journal of Marine Science and Technology* **22**: 574-586.
[36] Safaei A.A., Ghassemi H., Ghiasi M., 2018, Correcting and enriching vessel's noon report data using statistical and data mining methods, *European Transport \ TrasportiEuropei* **67**: 1-13.
[37] Whalley R., 1990, Interconnected spatially distributed systems, *Transactions of the Institute of Measurement and Control* **12**(5): 262-270.
[38] Whalley R., Bartlett H., Ebrahimi M., 1997, Analytical solution of distributed–lumped parameter network models. *Proceedings of the Institution of Mechanical Engineers - Part* I, *Journal of Systems and Control Engineering* **211**(I3): 203-218.
[39] Gholami A., Jazayeri S.A., Esmaili Q., 2020, Marine powertrain simulation for design and operational performance evaluation, *International Journal of Powertrains* **9**(4): 289-314.
[40] International Towing Tank Conference-Recommended Procedures and Guidelines, Preparation Conduct and Analysis of Speed/Power Trials, 7.5-04-01-01.1, Effective Date, Revision 05.
[41] Kim Y.D., Lee C.W., 1986, Finite element analysis of rotor bearing systems using a modal transformation matrix, *Journal of Sound and Vibration* **111**(3): 441-456.
[42] Ganta G., 2005, *Dynamics of Rotating Systems*, Springer, NY.
[43] DNVGL-CG-0038-Class Guideline - Calculation of Shafts in Marine Applications, Høvik, Norway.